

## Heat Capacity of Untwinned $\text{YBa}_2\text{Cu}_3\text{O}_{7-\delta}$ Crystals along the $H_{c2}$ Line

S. E. Inderhees, M. B. Salamon, J. P. Rice, and D. M. Ginsberg

Department of Physics and Materials Research Laboratory, University of Illinois at Urbana-Champaign,  
1110 West Green Street, Urbana, Illinois 61801

(Received 28 June 1990)

We report heat-capacity measurements on untwinned  $\text{YBa}_2\text{Cu}_3\text{O}_{7-\delta}$  single crystals in magnetic fields  $H \leq 7$  T, for both  $\mathbf{H} \parallel \mathbf{c}$  and  $\mathbf{H} \perp \mathbf{c}$ . Adding Gaussian fluctuations to a BCS-like step, we obtain a fit for  $H=0$ ,  $T \approx T_c$  that is consistent with a 3D, two-component order parameter in the strong-coupling limit. However, the  $H \neq 0$  data are inconsistent with this approach. A finite-size-scaling analysis, assuming critical behavior and an  $H$ -dependent length, satisfactorily describes the data.

PACS numbers: 74.30.Ek, 05.70.Jk, 74.40.+k, 74.70.Vy

Fluctuation effects are extremely difficult to observe in conventional superconductors,<sup>1</sup> but play predominant roles in the new high-temperature materials because of the extremely short low-temperature coherence length<sup>2</sup>  $\xi_0$ . We previously<sup>3</sup> presented evidence of fluctuation contributions to the heat capacity of  $\text{YBa}_2\text{Cu}_3\text{O}_{7-\delta}$  near  $T_c$ , and treated them in the Gaussian approximation. In this Letter, we report new data on largely untwinned single-crystal samples and consider the effect of external fields. The improved data, in zero field, still exhibit the temperature dependence expected from Gaussian fluctuations, but do not support our earlier conclusion that the number of order-parameter components must be larger than 2. However, the magnetic-field response<sup>4</sup> is inconsistent with the Gaussian approximation,<sup>5</sup> even when higher-order corrections are included.<sup>6</sup> In this Letter, we start with the observation that magnetic fields constrain the coherence length perpendicular to the applied field, and treat that constraint within the formalism of finite-size scaling (FSS).<sup>7</sup>

Millimeter-sized single crystals of  $\text{YBa}_2\text{Cu}_3\text{O}_{7-\delta}$  were grown at the University of Illinois using the CuO-rich technique described elsewhere.<sup>8</sup> Heat-capacity data from two samples (each with  $m \approx 40$   $\mu\text{g}$ ) are reported below. Sample YC187 contains a single untwinned domain accounting for approximately one-half of the total mass; the rest of the sample shows widely spaced twinning planes. Sample YC267 is approximately 85% single domain. Susceptibility measurements show both samples to display sharp transitions and low-temperature zero-field-cooled values near  $-1/4\pi$ . Heat-capacity measurements were performed using a standard ac method<sup>9</sup> described in detail elsewhere.<sup>10</sup> For measurements in field, a fine quartz fiber was varnished to one side of the sample to prevent rotation. Because the fiber was located more than a thermal diffusion length from the thermocouple, it did not change the observed heat-capacity signal.

Results for sample YC187 are plotted as  $C_p/T$  vs  $T$  in Fig. 1. Although the phonon heat capacity displays negative curvature in this temperature range, the data show positive curvature above and below  $T_c$ , attributable to

fluctuations. Data on sample YC267 in magnetic fields up to 7 T applied both parallel and perpendicular to the  $c$  axis are shown similarly in Fig. 2.

Fluctuation contributions to  $C_p$  can be treated as a correction to mean-field theory (MFT) if  $|t| \equiv |T/T_c - 1| \gg t_G$ , the reduced Ginzburg temperature. Estimates<sup>11,12</sup> of  $t_G T_c$  vary widely, from 0.1 to 10 K. For this reason, we fitted the zero-field data both by MFT plus Gaussian terms and by a critical (logarithmic) divergence. In the BCS theory, the MFT heat capacity below  $T_c$  is written<sup>13</sup>  $\Delta C_{\text{MF}} = a \gamma_{\text{eff}} T_c (1 + bt)$ , with  $a = 1.43$  and  $b = 1.92$  in the weak-coupling limit. Gaussian fluctuations contribute<sup>14</sup> a singular term  $C_{\text{fl}} = C_{\text{fl}}^{\pm}$

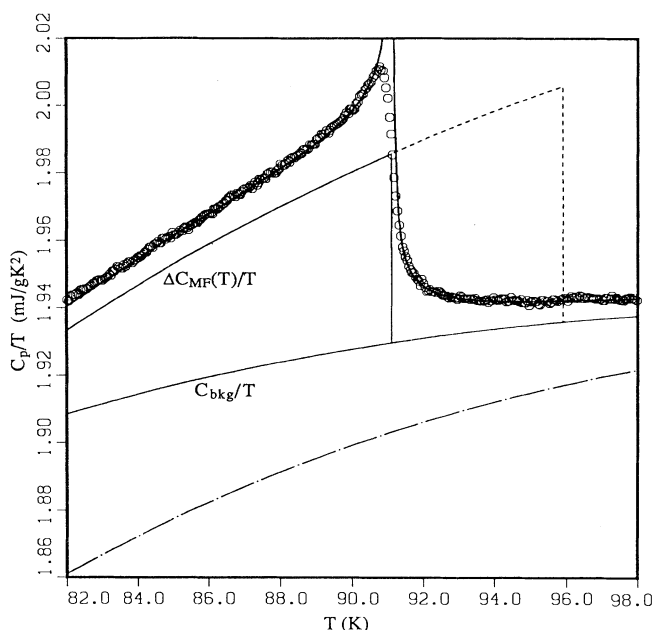


FIG. 1.  $C_p/T$  data and fitting function (solid line) for sample YC187, assuming  $\alpha = \frac{1}{2}$  and  $n=2$ . The dashed line is the result of an extrapolation of the mean-field step to account for the entropy of the fluctuations. The dot-dashed line indicates the background necessary to fit the data by a logarithmic divergence.

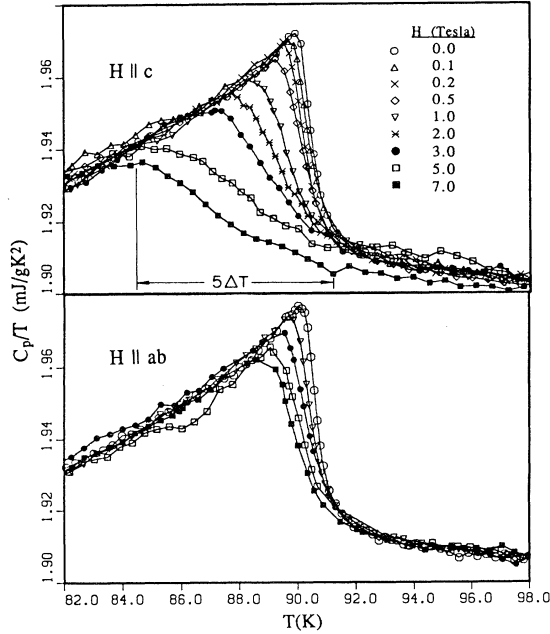


FIG. 2.  $C_p(H, T)/T$  for sample YC267, with  $H$  applied parallel to the  $c$  axis and parallel to the  $a$ - $b$  plane. The width factor  $5\Delta T$  that would approximately scale the 7-T data to the universal curve of Ref. 6 is indicated.

$\times |t|^{-\alpha}$ , where  $\alpha = (4-d)/2$ , and  $d$  is the dimensionality of the system. In 3D, for a Ginzburg-Landau theory with  $O(n)$  symmetry,  $C_{\bar{n}}^+$  is related to the geometric average of the coherence length  $\xi_0 = (\xi_a \xi_b \xi_c)^{1/3}$  through

$$C_{\bar{n}}^+ = nk_B / 16\pi \xi_0^3. \quad (1)$$

Here  $n$  is the number of real, independent components of the Ginzburg-Landau (GL) order parameter which is related<sup>15</sup> to the Gaussian amplitude ratio by  $n = 2^{d/2} C_{\bar{n}}^+ / C_{\bar{n}}^-$ . A value of  $n=2$  from this equation is not sufficient to establish  $s$ -wave pairing.<sup>3,16</sup>

To obtain sufficient precision, we approximate the lattice plus normal electronic contribution to  $C_p$  as a second-order polynomial, whose curvature near  $T_c$  is estimated by interpolating between values well above and below  $T_c$ . There are significant covariances among the adjustable parameters; the uncertainty in  $n$ , for example, derives primarily from that in  $T_c$  ( $90.9 \text{ K} < T_c < 91.2 \text{ K}$  for sample YC187). A systematic exploration of the  $\chi^2$  surface (fitting the data within  $T_c \pm 10 \text{ K}$  and excluding points very near  $T_c$ ) leads to the best fit shown in Fig. 1; with  $C_{\bar{n}}^+ = 0.14 \text{ mJ/gK}$ ,  $\alpha = \frac{1}{2}$ , and  $n=2$ , this leads to the value  $\xi_0 = 8.5 \text{ \AA}$ . The BCS step  $\Delta C_{\text{MF}}(T_c)$  is  $5.1 \text{ mJ/gK}$ . If we force  $\alpha=1$  (2D behavior), the resulting standard deviation is 50% higher and gives  $\xi_0 \approx 25 \text{ \AA}$ , substantially larger than other estimates. A fit by a logarithmic divergence gives  $\sigma \sim 30\%$  higher, and by  $n=6$ , 50% higher than the  $n=2$ ,  $\alpha = \frac{1}{2}$  best fit.

The fluctuation entropy arises because the observed  $T_c$  is reduced from the value  $T_c^{\text{MF}}$  which would obtain in the absence of fluctuations; we find  $T_c^{\text{MF}} = 95.9 \text{ K}$  by an equal-entropy construction. We use the extrapolated step  $\Delta C_{\text{MF}}(T_c^{\text{MF}}) = 6.6 \text{ mJ/gK}$  that describes the underlying MFT curve to find  $3.5 < b < 5.0$ , within the range expected for strong-coupling superconductors.<sup>17</sup> The uncertainty in  $b$  reflects that in the curvature of the lattice term.

In a magnetic field, electrons in the lowest-order Landau orbit are the first to undergo a transition at  $T_c(H)$ . This limits the coherence length perpendicular to the applied field ( $\xi^\perp$ ) to the Landau radius  $a_0 = (\phi_0 / 2\pi H)^{1/2}$ , where  $\phi_0$  is the flux quantum. As Lee and Shenoy<sup>5</sup> pointed out, the field thereby reduces the effective dimensionality from  $d=3$  to  $d=1$ , and leads to a broadening of the transition. Thouless<sup>6</sup> and others have extended this 1D analysis to obtain curves of constant height that can be superposed by locating  $T_c(H)$  and the point of maximum upward curvature and scaling the temperature axis by a width parameter  $\Delta T(H)$  (where  $n=2$  is assumed):

$$\frac{\Delta T(H)}{T_c(H)} = \left[ \frac{C_{\bar{n}}^+}{\Delta C_{\text{MF}}(T_c)} \right]^{2/3} \left[ \frac{T_c(0) - T_c(H)}{T_c(H)} \right]^{2/3}. \quad (2)$$

The shift  $T_c(0) - T_c(H)$  is proportional to  $H$ , and the point of maximum downward curvature occurs approximately  $5\Delta T$  below  $T_c(H)$ . Our data (Fig. 2) indicate that  $T_c(H)$  thus defined is barely shifted in field, certainly by less than 1 K, while  $5\Delta T \approx 7 \text{ K}$ , both in a 7-T field parallel to the  $c$  axis. Taking  $T_c(0) - T_c(H) < 1 \text{ K}$  implies  $C_{\bar{n}}^+ / \Delta C_{\text{MF}}(T_c) > 0.18$ , whereas we find 0.0027 from our zero-field MFT analysis. It is interesting to note that  $t_G$  may be expressed  $t_G \approx 2[C_{\bar{n}}^+ / \Delta C_{\text{MF}}(T_c)]^2$ . The data thus imply that  $t_G T_c > 5.5 \text{ K}$ , indicating that the 1D mean-field approach is not self-consistent. We must consider, then, critical-point effects.

If the coherence length of a system undergoing a phase transition is limited by the finite size  $L$  of the system, its heat capacity can be related<sup>18</sup> to the critical divergence of the infinite system by the substitution

$$t \rightarrow t^* = [(t + \delta_L)^2 + (\Delta_L)^2]^{1/2}, \quad (3)$$

where  $\delta_L$  and  $\Delta_L$  parametrize the size-dependent shift and broadening, and it is assumed that there is no phase transition in the finite system. Scaling arguments<sup>7</sup> suggest that  $\delta_L \propto (\xi_0/L)^\lambda$  and  $\Delta_L \propto (\xi_0/L)^\nu$ , where  $\lambda = \theta = 1/\nu$ . The length that plays the role of  $L$  here is clearly<sup>5,6</sup>  $a_0(H)$ , so that

$$\delta_H \sim \Delta_H \sim [2\pi(\xi_0^\perp)^2 H / \phi_0]^{1/2\nu}. \quad (4)$$

Dasgupta and Halperin<sup>19</sup> exploited FSS to analyze the Monte Carlo simulation of a lattice superconductor of size  $L^3$ . A key result is the observation that the heat-capacity maximum  $\Delta C_m(L)$  grows logarithmically with

system size  $L$ . We parallel this approach by writing

$$\Delta C(T, H) = \frac{-A}{2} \ln[(t + \delta_H)^2 + (\Delta_H)^2] + \frac{D}{2} \operatorname{erfc}\left[\frac{t + \delta_H}{\Delta_H}\right]. \quad (5)$$

The complementary error function permits a broadened step in addition to the logarithmic singularity. Because of the step, this function has a maximum at  $t_m = -\delta_H - y_0 \Delta_H$ , where  $y_0$  depends on the ratio  $D/A$ . In terms of the variable  $y = (t - t_m)/\Delta_H$ , Eq. (5) may be written as

$$\Delta C_m(H) - \Delta C(T, H) = \frac{A}{2} \ln\left[\frac{1 + (y - y_0)^2}{1 + (y_0)^2}\right] + \frac{D}{2} [\operatorname{erfc}(-y_0) - \operatorname{erfc}(y - y_0)], \quad (6)$$

with

$$\Delta C_m(H) = -A \ln(\Delta_H) - \frac{A}{2} \ln[1 + (y_0)^2] + \frac{D}{2} \operatorname{erfc}(-y_0).$$

We test this scaling hypothesis in Fig. 3 by plotting

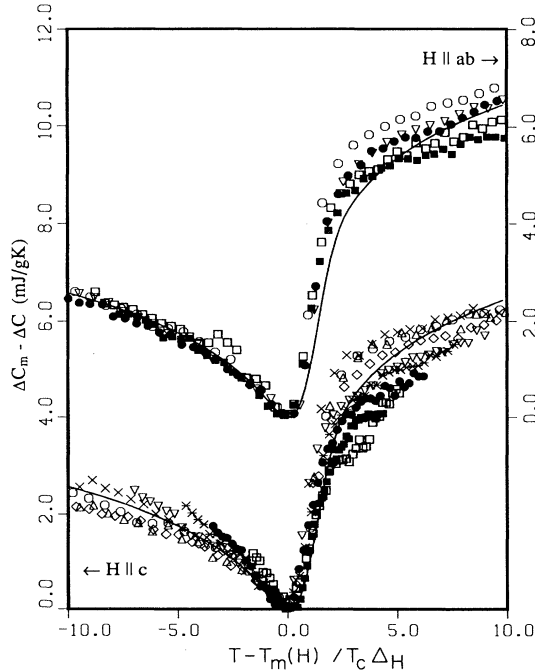


FIG. 3. Scaled heat-capacity data of sample YC267. The data are plotted as the difference between the electronic heat capacity and the maximum  $\Delta C_m(H)$  vs scaled temperature. The solid line represents the fit of the data by Eq. (6).

the data of Fig. 2 in the form  $\Delta C_m(H) - \Delta C(T, H)$  vs  $y = [T - T_m(H)]/T_c \Delta_H$ . The parameters  $\Delta C_m$ ,  $T_m$ , and  $\Delta_H$  are chosen for each data set to collapse all data to a single curve. To be consistent, we subtract the background heat capacity determined from fitting a logarithmic divergence to the zero-field data, although the magnitude of this cancels in the scaling procedure. The solid line is a plot of Eq. (6) for  $A = 1.3$  mJ/gK and  $D = 4.2$  mJ/gK, for which  $y_0 = 1.14$ .

Figure 4(a) shows the logarithmic relationship between  $\Delta C_m(H)$  and the  $\Delta_H$  used to scale the data in Fig. 3. Because the zero-field data are also rounded, we assume the zero-field broadening is due to an inhomogeneity length scale  $L_0$  that adds in quadrature to the field-dependent width; i.e.,  $\Delta_H^2 = \Delta_0^2 + \Delta_f^2$ , where

$$\Delta_0^2 = \left(\frac{\xi_0}{L_0}\right)^{2/\nu} \quad \text{and} \quad \Delta_f^2 = \left[\frac{2\pi(\xi_0^\perp)^2}{\phi_0} H\right]^{1/\nu}. \quad (7)$$

$\Delta_H^2$  is plotted versus  $H^{3/2}$  ( $\nu = \frac{2}{3}$ ) in Fig. 4(b). The intercept and slopes indicate  $L_0 \approx 30\xi_0$ ,  $\xi_0 \approx 1.5$  Å, and  $\xi_0^{\perp} \approx 7$  Å. There could certainly be numerical factors in the definition of  $\Delta_f$  that change the absolute values. Note that  $\nu = \frac{2}{3}$  is consistent with a logarithmic heat-capacity singularity ( $\alpha = 0$ ).

Based on the similarities of the data in fields to calculations for superconducting particles, de Jongh<sup>20</sup> attributed the size limit to dislocations in the flux-line lattice.

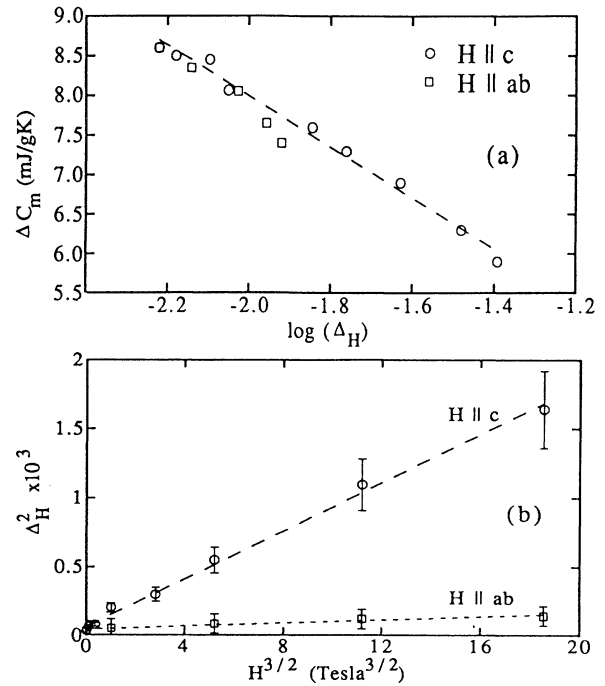


FIG. 4. (a) Suppression of the heat-capacity maximum  $\Delta C_m(H)$  logarithmically with increasing transition width  $\Delta_H$ . (b) Broadening of the transition with increasing field  $H$ .

We suggest here that the more fundamental constraint on  $\xi^{\pm}$ , induced by the field, is by itself capable of producing finite-size effects. Recently, Wohlleben *et al.*<sup>21</sup> have fitted polycrystalline data on  $\text{YBa}_2\text{Cu}_3\text{O}_{7-\delta}$  by a logarithmic divergence with similar amplitudes to those found here. Even if the zero-field data are in the crossover regime, the critical region is expanded by an applied field,<sup>5</sup> making the finite-size scaling analysis the more appropriate approach. Further, unlike the mean-field result, it satisfactorily fits all the data presented here.

We have benefited from the suggestions of Nigel Goldenfeld regarding field-dependent length scales. This work was supported through the University of Illinois Materials Research Laboratory by NSF Grant No. DMR 89-20538 and by NSF Grant No. DMR 87-14555.

<sup>1</sup>W. J. Skocpol and M. Tinkham, Rep. Prog. Phys. **38**, 1049 (1975).

<sup>2</sup>R. J. Cava *et al.*, Phys. Rev. Lett. **58**, 1676 (1987).

<sup>3</sup>S. E. Inderhees, M. B. Salamon, N. Goldenfeld, J. P. Rice, B. G. Pazol, and D. M. Ginsberg, Phys. Rev. Lett. **60**, 1178 (1988).

<sup>4</sup>M. B. Salamon, S. E. Inderhees, J. P. Rice, B. G. Pazol, D. M. Ginsberg, and N. Goldenfeld, Phys. Rev. B **38**, 885 (1988).

<sup>5</sup>P. A. Lee and S. R. Shenoy, Phys. Rev. Lett. **28**, 1025 (1972).

<sup>6</sup>D. J. Thouless, Phys. Rev. Lett. **34**, 946 (1975); G. J. Ruggeri and D. Thouless, J. Phys. F **6**, 2063 (1976).

<sup>7</sup>M. E. Fisher and M. N. Barber, Phys. Rev. Lett. **28**, 1516 (1972).

<sup>8</sup>J. P. Rice, B. G. Pazol, D. M. Ginsberg, T. J. Moran, and M. B. Weissman, J. Low Temp. Phys. **72**, 345 (1988).

<sup>9</sup>P. Sullivan and G. Seidel, Phys. Rev. **173**, 679 (1968).

<sup>10</sup>S. E. Inderhees, Ph.D. Dissertation, University of Illinois, 1990 (unpublished).

<sup>11</sup>C. J. Lobb, Phys. Rev. B **36**, 3930 (1987).

<sup>12</sup>D. S. Fisher, M. P. A. Fisher, and D. A. Huse (to be published).

<sup>13</sup>A. A. Abrikosov, L. P. Gorkov, and I. E. Dzyaloshinski, *Methods of Quantum Field Theory in Statistical Physics* (Dover, New York, 1963), p. 306.

<sup>14</sup>R. A. Ferrell, J. Low Temp. Phys. **1**, 241 (1969).

<sup>15</sup>S.-k. Ma, *Modern Theory of Critical Phenomena* (Benjamin, Reading, MA, 1976).

<sup>16</sup>J. Annett, M. Randeria, and S. R. Renn, Phys. Rev. B **38**, 4660 (1988).

<sup>17</sup>R. Akis, F. Marsiglio, and J. P. Carbotte, Phys. Rev. Lett. **47**, 1556 (1981).

<sup>18</sup>M. E. Fisher and A. E. Ferdinand, Phys. Rev. Lett. **19**, 169 (1967).

<sup>19</sup>C. Dasgupta and B. I. Halperin, Phys. Rev. Lett. **47**, 1556 (1981).

<sup>20</sup>L. J. de Jongh, Solid State Commun. **70**, 955 (1989).

<sup>21</sup>D. Wohlleben, E. Braun, W. Schnelle, J. Harnischmacher, S. Rupper, and R. Dómel (to be published).